## ORIGINAL PAPER

**Brian Jackson · Steve Harper ·
Laura Smith · Jane Flinn**

# Elemental mapping and quantitative analysis of Cu, Zn, and Fe in rat brain sections by laser ablation ICP-MS

**Abstract** This report details the application of laser ablation quadrupole ICP-MS for the (multi)elemental mapping of 100-µm-thick sections of rat brain. The laser spot size used was 60 µm, and the laser scan speed was 120 µm s$^{-1}$. The analysis was relatively rapid, allowing mapping of a whole brain thin section ($\approx$1 cm$^2$) in about 2 h. Furthermore, the method was amenable to multi-element data collection including the physiologically important elements P and S and afforded sub µg g$^{-1}$ detection limits for the important trace elements Cu and Zn. Calibrations were performed with pressed pellets of biological certified reference materials, and the elemental distributions and concentrations of Cu, Zn, and Fe were determined in whole rat brain sections. The distributions and concentration ranges for these elements were consistent with previous studies and demonstrate the utility of this technique for rapid mapping of brain thin sections.

**Keywords** Laser ablation ICP-MS · Rat brain sections · Elemental imaging

B. Jackson ($\boxtimes$)
Departments of Earth Sciences and Chemistry,
Dartmouth College,
Hanover, NH 03755, USA
e-mail: Brian.P.Jackson@dartmouth.edu
Tel.: +1-603-16461272

S. Harper
Savannah River Ecology Laboratory,
University of Georgia,
Aiken, SC 29802, USA

L. Smith · J. Flinn
Department of Psychology,
George Mason University,
4400 University Drive,
Fairfax, VA 22030, USA

## Introduction

In studies of the chemistry and biology of inorganic elements in biological systems, it is often necessary to know both the concentration and the spatial distribution of the element within cells, tissues, and organs. A number of complementary analytical techniques exist for the mapping of elemental distributions in biological tissues; some offer excellent resolution at the expense of higher detection limits, whereas others afford lower detection limits but at the expense of lower resolution. The required rigor of sample preparation, conditions of analysis (i.e., pressure, temperature, and hydration conditions), availability and expense of required instrumentation, and range of analytes that can be determined must also be considered when selecting an analytical technique. The most widely applied surface analytical techniques for elemental imaging in biological tissues are transmission electron microscopy with energy dispersive X-ray analysis (TEM-EDX), proton-induced X-ray emission (PIXE), and secondary ion mass spectrometry (SIMS). Comprehensive reviews of TEM-EDX [1], PIXE [2], and SIMS [3] and their application to biological samples are available. Increasingly, synchrotron X-ray absorption spectroscopy (SXAS) is being used for the multi-elemental imaging in biological thin sections [4]. In SXAS, the incident X-ray penetrates the whole thickness of the tissue section: the resultant elemental concentrations and elemental images are therefore volume averaged and not necessarily representative of the surface of the thin section. These analytical techniques provide sub-micron resolution with detection limits generally < 100 mg kg$^{-1}$, and in some cases <10 mg kg$^{-1}$.

Laser ablation inductively coupled plasma mass spectrometry (LA-ICP-MS) is well established as a microprobe for elemental mapping in the geological sciences and has been applied to biological tissues such as plant leaves [5, 6], snake tails [7], bivalve shells [8–10], and tree rings [11–13]. The application of LA-ICP-MS to analysis of fresh hydrated liver samples using a cryogenically cooled ablation cell has been demonstrated [14, 15]. The Becker research group has recently demonstrated that LA-ICP-MS

can be used to image elemental distributions in human and rat brain thin sections utilizing a cryo-cooled laser ablation chamber and a double-focusing sector field ICP-MS [16, 17]. The recent applications of LA-ICP-MS to biological samples have been reviewed [18].

In this study we report on the application of quadrupole LA-ICP-MS for the two-dimensional (2D) elemental mapping of rat brain sections. Metal ions such as Zn, Cu, Fe, Ca, and Al have been implicated in neurological disorders such as Parkinson's disease, epilepsy, and Alzheimer's disease [19, 20], and SXAS and PIXE have previously been used to study the distribution of such elements in brain thin sections [21–24]. LA-ICP-MS has been used to study P and metal-containing proteins from brain tissue by the analysis of 2D PAGE gels [25, 26]. Flinn et al. have used synchrotron microprobe XRF to generate 2D elemental maps of rat brain sections [4]. While this analytical technique generates high quality data, access to synchrotron facilities is limited and competitive, and the methodology requires relatively long dwell times per pixel to achieve suitable detection limits once beamtime is obtained. This limits the number of samples that can be analyzed, reduces the spatial extent that can be examined, or necessitates that relatively long step lengths be used in the X and Y dimensions, which reduces the resolution of the resultant elemental map and leaves areas of the sample unanalyzed.

The present study explores the use of LA-ICP-MS as a complement to the SXAS work. The primary objective was to develop methodology that allows for the quantitative determination of spatial distributions of multiple elements in whole brain sections within a relatively short (2–3 h) analysis time and with low detection limits. Accurate quantitative analysis by LA-ICP-MS is a challenge because of the lack of suitable certified solid standards. Various calibration procedures have been used for LA-ICP-MS and perhaps the most accurate approach is to have true matrix matching of standards and samples [7, 16]. Commercially available certified reference materials have also been used for calibration of LA-ICP-MS [14], and that approach was used for this study. The work reported herein also complements that of Becker et al. [16, 17] and illustrates the application of a quadrupole ICP-MS and regular laser ablation chamber to obtain elemental maps of whole rat brain thin sections (i.e., approximately 1 cm$^2$).

## Materials and Methods

### Instrumentation

A UP213 laser ablation system (New wave, CA) interfaced with an Elan 6100 DRC plus ICP-MS (Perkin Elmer, Shelton, CT) was used throughout this work. General operating conditions for LA-ICP-MS are given in Table 1. The lens voltage and carrier gas flow rate were optimized daily by ablating a pressed pellet of the lobster hepatopancreas certified reference material TORT-2 (NRC, Ottawa,

**Table 1** laser ablation and ICP-MS operating parameters

| Parameters | Value |
|---|---|
| **ICP-MS parameters** | |
| Plasma flow rate (L min$^{-1}$) | 15 |
| Auxilliary flow rate (L min$^{-1}$) | 1.2 |
| Carrier flow rate (L min$^{-1}$) | 1 |
| Lens voltage (V) | 6 |
| Isotopes ($m/z$) | $^{12}$C, $^{13}$C, $^{24}$Mg, $^{26}$Mg, $^{39}$K, $^{43}$Ca, $^{44}$Ca, $^{56}$Fe, $^{63}$Cu, $^{65}$Cu, $^{66}$Zn, $^{68}$Zn |
| Dwell time/ $m/z$ (ms) | 45 (20 and 40 for $^{12}$C and $^{13}$C, respectively) |
| Read time/replicate (s) | 0.5 |
| Readings/replicate | 185 |
| Replicate time (s) | 92.5 |
| **Laser ablation parameters** | |
| Wavelength (nm) | 213 |
| Frequency (Hz) | 10 |
| Spot size (μm) | 60 |
| Laser power (J cm$^{-2}$) | 1.78 |
| **2D multiline scan set up** | |
| Average X scan length (μm) | 10,000 |
| Scan rate/sec (μm s$^{-1}$) | 120 |
| Distance between line scans in Y (μm) | 100 |
| No of line scans per thin section | 70–95 |

Canada). Laser power and spot size were optimized by rastering a 100-μm rat brain section. Laser output power was kept at <70% to prevent ablation through the entire tissue section. Background readings were <30 cps for all elements except $^{56}$Fe (blank values 8,000-12,000 cps) which was due to ArO$^+$. Polyatomic interferences are possible for the other analytes: therefore multiple isotopes were monitored for each element and the abundance ratios were compared with the natural abundance values. Initial qualitative experiments were conducted (i.e., no calibration was performed) to assess signal stability and sample integrity over an extended period for a range of analytes (study 1). An additional set of brain thin sections was analyzed for a reduced suite of analytes and, in this case, quantitative analysis was performed (study 2).

The maximum dimensions of each brain thin section was determined using the CCD display and laser ablation software. Thin sections were approximately 10,000-μm wide and 7,000- to 9,500-μm long. A line scan was drawn in the X dimension from top left to top right of the desired scan area, using line scan laser properties as specified in Table 1. This line was then copied and pasted in the Y dimension using the duplicate scan software feature with an inter-line step size of 100 μm; the number of copies was

between 70 and 95 depending on the dimensions of the given thin section. The scan speed of each line was 120 μm s$^{-1}$, and the ICP-MS was configured in data-only mode to collect 185 readings per line scan at a rate of 2 s$^{-1}$. Each laser line scan was recorded as an individual ICP-MS data file, and data collection was initiated automatically using the relay signal from the laser ablation software. In this manner up to seven brain sections were placed on a microscope slide, loaded in the ablation cell; the analysis grid for each was defined using laser ablation software and corresponding sample IDs were defined using ICP-MS software. This then permitted up to 20 h of automated sample analysis.

Sample preparation

Coronal brain sections were prepared from male Sprague–Dawley rats, aged 12 months in Study 1 and six months in Study 2 (12-month-old animals have higher levels of Fe). Rats were anaesthetized by intraperitoneal (IP) injection of tribromoethanol and then sacrificed for immediate brain extraction. Since optimal section thickness was initially under investigation, Study 1 examined sections of both fixed and unfixed tissue at varying thickness. Fresh frozen tissue was sliced using a cryostat at 99 μm (Sakura Finetek, Tissue-Tek Cryo$_3$, Torrance, CA). Fixed tissue was prepared using both the cryostat (99 μm) and a vibratome (The Vibratome Company, 1000 Plus, St. Louis, MO; 100, 120, and 150 μm). In Study 2, sections were prepared at 99 μm from fresh frozen and fixed tissue. In both studies, satisfactory data was obtained using cryostat sections of 99 μm for both fixed and unfixed tissue. Sections in both studies were mounted on two-inch glass slides without coverslips and were allowed to air dry at room temperature for less than a week prior to LA ICP-MS. In Study 2, the slides were pre-coated with gelatin (subbed) to increase the adhesion of the tissue to the slides. Tissue was fixed either by saline perfusion followed by 4% paraformaldehyde or by immersing a bisected brain (with cerebellum removed) in a 4% paraformaldehyde solution. Paraformaldehyde solutions were diluted with 0.9% dH$_2$O saline.

## Calibration Standards

Pressed pellets of the certified reference standards TORT-2, DOLT-2, and DORM-2 (NRC, Ottawa, Canada) were prepared with approximately 100 mg of the material using a Carver laboratory press at $15 \times 10^5$ Pa for 5 min. The pellets were affixed to a microscope slide and line scans (3 per standard) were ablated using the laser and ICP-MS data collection parameters outlined above. Three gas blank line scans were performed with 0% laser power. Individual readings within a line scan were averaged and the 3 lines were used as replicate measurements in the calibration regression equations.

Data analysis and visualization

ICP-MS data files for each brain thin section were labeled consecutively and output as a comma delimited text file of element intensity over time. Each data row within this file corresponded to a 60-μm step size in the X dimension, while consecutive files corresponded to a 100 μm step size in the Y dimension. Using a simple text editing script, appropriate Y dimension values were added to each record within each line scan file, and then all line scans generated for a thin section were concatenated to a single file. Spatially explicit information for each element was then imported as point data and converted to a continuous raster surface using ArcGIS (version 8.3, ESRI). Localized areas where elements were concentrated could be readily visualized by their contrasting color in color-ramped 2D maps and as surface peaks in 3D models.

## Results and discussion

Previous analysis of rat brain thin sections by SXRF has shown that localized areas of Cu, Zn, and Fe can be detected in brain thin sections of rats [4] and these areas were of the order of 100–300 μm. We hypothesized that an LA-ICP-MS method with rapid scanning and a somewhat increased beam size would allow whole brain thin sections to be scanned in a reasonable time, on the order of hours, with comparable detection limits to SXRF, albeit with a reduction of spatial resolution.

The beam size of the UP213 laser ablation system can be imaged as low as 5 μm for the highest spatial resolution; however, under these conditions a relatively small amount of material reaches the ICP-MS, and hence detection limits are relatively high. Additionally, such a small beam size would lead to longer scan times, smaller step sizes, and longer analysis times. It was determined that a beam diameter of 40–60 μm would provide adequate resolution and allow for analysis of the whole brain section. As would be expected from the increase in ablation area, increasing the laser spot size from 40 μm to 60 μm doubled the signal intensity for analytes. Varying laser power had less effect on analyte signal intensity; however 70% laser power, corresponding to 1.78 J cm$^{-2}$, increased signal intensity for Mg and Fe, whereas, from visual inspection, this laser power did not ablate through the brain section.

LA-ICP-MS can provide data for light elements such as Mg and Al and this is of significance for mapping brain tissue, given the potential involvement of Al in Alzheimer's disease. Because O$_2$ is essentially absent from the LA-ICP-MS sample introduction system, low background at $m/z$ 56 can be obtained as compared to normal solution nebulization where dissolved O$_2$ and H$_2$O are ubiquitous and result in very high background $^{40}Ar^{16}O^+$ interference at $m/z$ 56. Thus it is possible to monitor $^{56}$Fe under standard (non-reaction cell) conditions, which is important because this Fe isotope is 92% abundant.

The low $O_2$ concentration of the carrier also suggested that other non-traditional (for quadrupole ICP-MS) isotopes such as $^{31}P$ and $^{32}S$ may be amenable to analysis by LA-ICP-MS, and indeed 2D elemental mapping of these elements indicated their ubiquitous presence in brain tissue and, for P, areas of differential concentration (Fig. 1). Analysis of these elements by LA-ICP-MS could be used to determine areas of increased phosphorylation or high concentrations of sulphydryl-rich proteins in biological tissues. A caveat to the analysis of isotopes with oxygen-based polyatomic interferences is that background values are increased upon opening the sample cell and then decrease to background levels for some time after re-closing the cell. Additionally, O-rich areas of the sample would give false positives for these isotopes; although in this case, as with C, we assume that the O concentration of biological tissue is homogeneously distributed.

The elemental distribution shown in Fig. 1, which shows a 120-µm-thick coronal section from the caudal hippocampal region of a 12-month-old rat, approximately Bregma-6.3 [27], prepared by immersion in 4% paraformaldehyde, illustrates the utility of the LA-ICP-MS technique. As would be expected $^{13}C$, $^{32}S$, and $^{31}P$ are present throughout the brain tissue at high concentrations, while $^{56}Fe$ and $^{63}Cu$ have distinct areas of localization. $^{56}Fe$ is seen in the dentate gyrus (DG) of the hippocampus and in the substantia nigra (SN). $^{63}Cu$ is seen in the medial geniculate nucleus (MGN), part of the superior colliculus (SC), and the periaqueductal grey (PAG). $^{66}Zn$ does not display localized areas of concentration in this section, but does so in the more rostral section containing the hilus of the hippocampus (Fig. 3, see later discussion).

The second set of analyses (study 2) provided quantitative data on a limited suite of elements (Fe, Cu, Zn) in a series of seven consecutive rat brain sections, and allowed us to examine signal stability over the duration of analysis (approximately 20 h). Coronal sections of fixed tissue taken at regular intervals (excluding the cerebellum), approximately 1 mm apart were used. Calibration curves were constructed using pressed pellets of biological certified reference materials. In general excellent linearity was obtained for these elements over four calibrations on consecutive days (Fig. 2). $R^2$ values were >0.98 for each element over the four calibrations, with the poorest linearity obtained for $^{56}Fe$, where DORM-2 repeatedly recorded lower signal intensity than TORT-2 despite its higher certified concentration (142 mg kg$^{-1}$ compared with 105 mg kg$^{-1}$ for TORT-2). This may be due to specific interferences for TORT-2, perhaps formation of $^{40}Ca^{16}O$ leading to increased signal intensity at $m/z$ 56. Alternatively, DORM-2 has high certified concentrations for Cr and Ni for a fish muscle sample and it is thought that these concentrations arise from stainless steel contamination during the reference material preparation stage, in which case a significant portion of the Fe in DORM-2 might arise from this contamination and this Fe phase could conceivably ablate differently than 'biological' Fe. It is also possible that air was entrained into the calibration standard during the pressing of DORM-2 into a pellet. This could have led to a false positive signal caused by ArO$^+$ at $m/z$ 56.
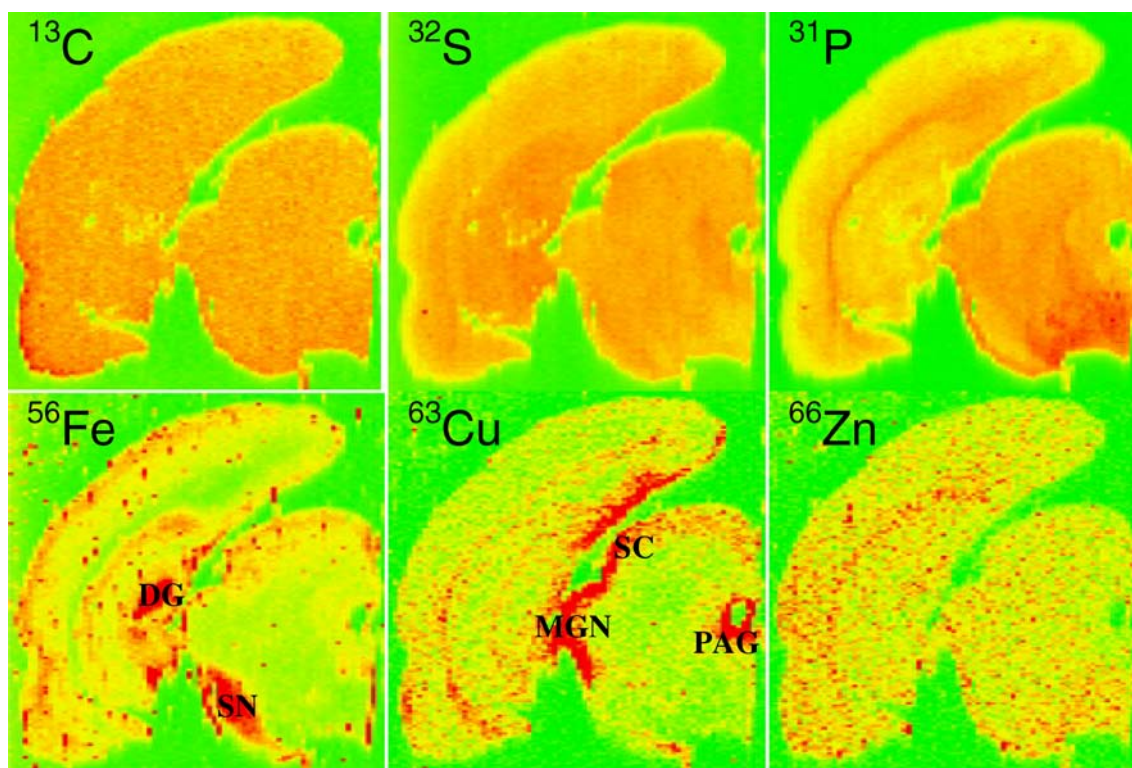


**Fig. 1** Qualitative elemental maps for whole rat brain sections. See text for an explanation of abbreviations
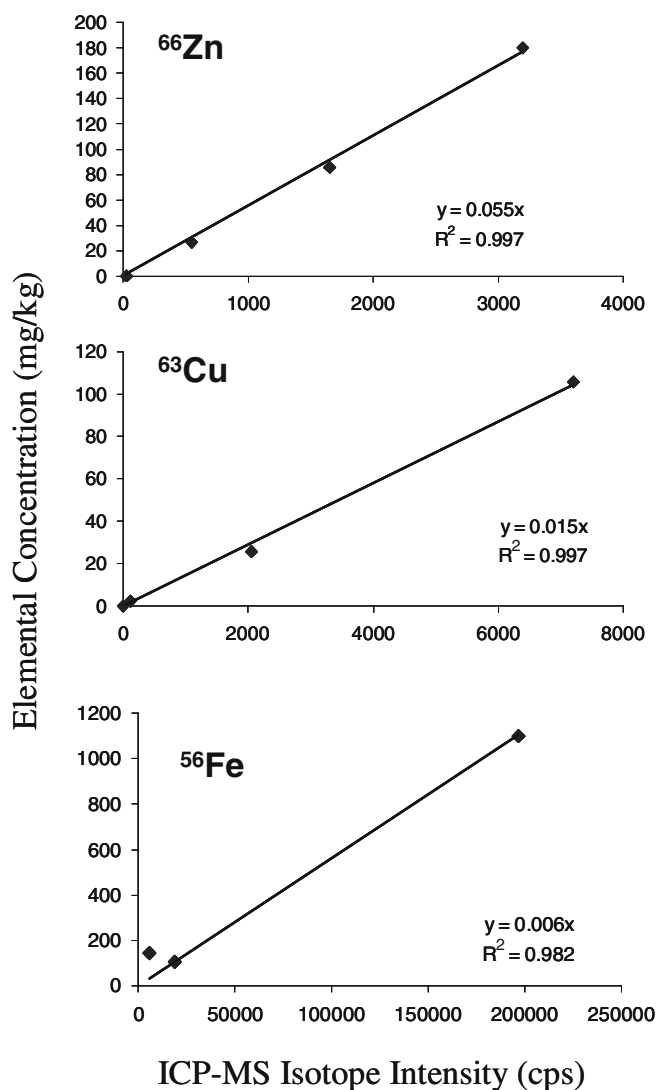
**Fig. 2** Representative calibration curves employing pressed pellets of TORT-2, DORM-2, and DOLT-2 certified reference materials

the $^{13}$C signal, which behaved identically) is not a good indicator of how signal intensities of other analytes vary for these standards; that is, it would not be an effective internal standard because its value remained relatively constant for all standards, while other analyte signals varied significantly between calibration dates. For this reason, calibration curves were constructed without referencing analyte responses to an internal standard intensity.

Average detection limits for the three analytes, calculated as $3\sigma$ of the blank measurements, were 3.6, 0.12, and 0.66 µg g$^{-1}$ for $^{56}$Fe, $^{63}$Cu, and $^{66}$Zn respectively, with the higher value for Fe reflecting the larger variation in blank values for this element due to the ArO$^+$ interference. Robertson et al. [24] used a similar LA-ICP-MS setup to this study and reported detection limits for Cu of 0.3 mg kg$^{-1}$ and a precision of 9.6% rsd using a 20-µm laser spot size for a 20-µm synthetic section standard; they also reported that LA-ICP-MS may provide better detection limits than micro-PIXE for heavier elements such as Pb or Hg. Detection limits for Cu and Zn in soft tissue using a cryo-cooled laser ablation cell and a time of flight ICP-MS were 0.05 and 0.02 mg kg$^{-1}$, respectively, using a 200-µm spot size [14] and reported precision was 2–6% rsd. The detection limits and precision reported in our study are, therefore, comparable to these two previous soft tissue LA-ICP-MS studies. Clearly, detection limits for LA-ICP-MS are primarily a function of the laser spot size, which, as previously stated, can be increased to achieve lower detection limits at the expense of reduced resolution.

Elemental concentrations in rat brain sections

Figure 3 (a–c, respectively) shows the distribution of Fe, Cu, and Zn in a section at approximately Bregma −4.0 mm [27] together with an adjacent brain section stained with thionine (Fig. 3d). Of note are the regions showing greatest Zn, Fe, and Cu concentrations. Zinc appears highest in CA2, CA3, and CA4 (hilus) of the hippocampus (HC) with the highest concentrations being in the hilus (HI), consistent with previous measurements [28]. High levels are also seen in the lateral amygdala (LA), a number of olfactory amygdalar nuclei (OlfA), and in cortical regions, including Parietal 1 and 2 (PAR1 & 2) and pyriform cortex (PC). Copper shares one region of high concentration with Zn, the LA, but is also high in dorsomedial aspect of the diencephalon (DMD). Iron also appears to be at its highest concentration in the hippocampus but is localized within the dentate gyrus (DG) where Zn values are very low. It is also seen in the caudate putamen (CP). Like Zn, Fe is also found in PAR1 and 2.

A number of different methods have been used to examine the concentrations of metals in human and rodent brain: these include ICP-MS, stable-isotope dilution mass spectrometry (SIDMS), atomic absorption spectrometry, and instrumental neutron activation analysis. Both wet and dry tissues have been examined, with dry values being approximately 4.5 times wet values; many of these results for human brain tissue have been reviewed by Speziali and

The precision of measurement calculated by averaging the individual relative standard deviation (rsd) for each standard over the four calibrations was 2.7%, 7.5%, 12.5%, and 6.7% for $^{12}$C, $^{56}$Fe, $^{63}$Cu, and $^{66}$Zn, respectively; the rsd for Cu improved to 8.7% when DORM-2 (Cu concentration of 2.34 mg kg$^{-1}$) was omitted. While these rsd values are above those expected for solution analysis, they are deemed acceptable for laser ablation sample introduction where sample inhomogeneities, differences in laser coupling between samples, and variation in ablated particle size can affect the precision of measurement. The $^{12}$C rsd for the mean signal intensity of each SRM averaged between the four calibration days was 12.5%, 9.5%, and 9.6% for TORT-2, DORM-2, and DOLT-2 respectively. However, when rsds for Fe, Cu, and Zn are compared between calibration days the values were substantially greater, 49.3%, 41.8%, and 33.8% for Fe, Cu, and Zn, respectively, despite the good linearity, as indicated by high $R^2$ values for calibration curves, on any given analysis day. This suggest that the $^{12}$C signal (or

956

**Fig. 3** Quantitative elemental distribution maps for Fe (**a**), Cu (**b**), and Zn (**c**), compared with an optical image of the adjacent thionine-stained section (**d**). Concentrations for hotspots and the appropriate physiological region are indicated (see text for an explanation of abbreviations)
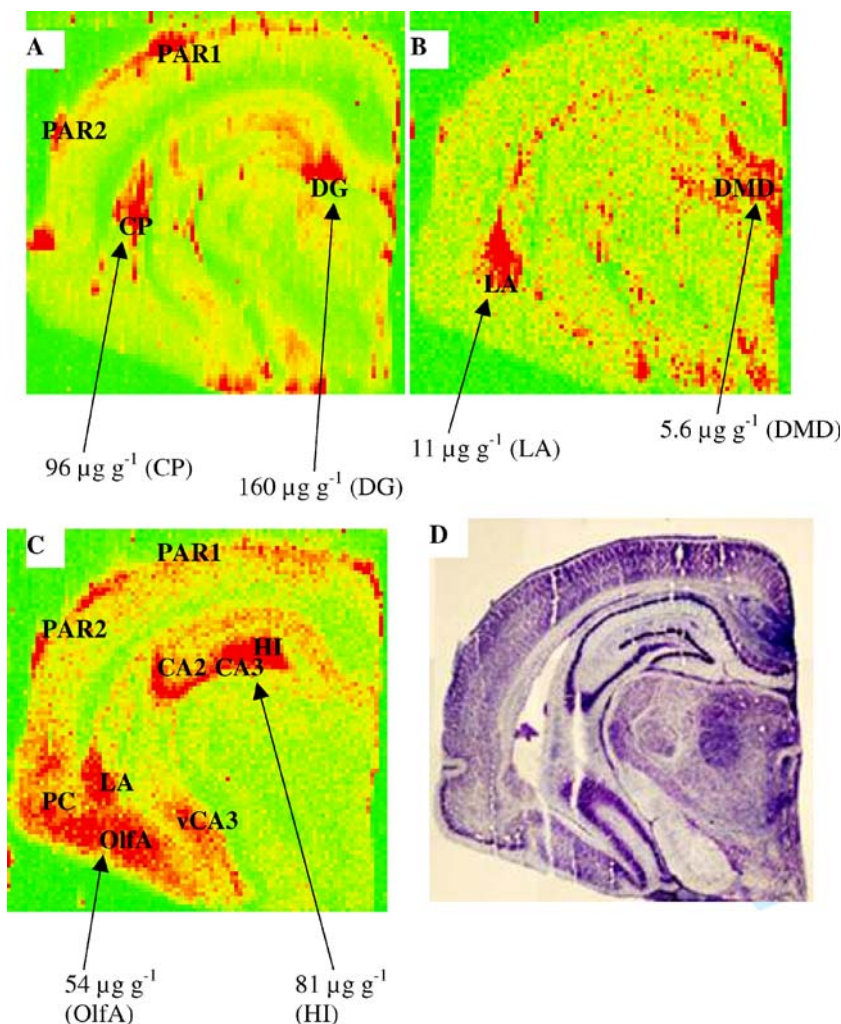


Orvini [29]. The average values reported for dry hippocampal tissue are 15, 70, and 216 $\mu g\ g^{-1}$ for Cu, Zn, and Fe, respectively (excluding one outlying iron value). Frederickson [30] used SIDMS to obtain values of 102–145 $\mu g\ g^{-1}$ for dry weight Zn in the hilar region of the rat hippocampus. Tarohda [31] recently used ICP MS to obtain wet values of 3, 35, and 25 $\mu g\ g^{-1}$ for Cu, Zn, and Fe in the hippocampus of 5-month-old rats. Hence the concentrations reported in this study, of 11, 81, and 160 $\mu g\ g^{-1}$, for Cu, Zn, and Fe respectively, are consistent with previous studies.

## Conclusions

This study has illustrated that quadrupole LA-ICP-MS provides sensitive detection and rapid spatial analysis of biological thin sections generating multiple-2D elemental maps. This technique can be useful in identifying areas of elemental localization in itself and as a precursor to more in-depth studies using synchrotron X-ray techniques, either to map the area at higher spatial resolution or to discern the in situ chemical speciation of the trace element. The location of hotspots and the measured concentrations of Fe,

Cu, and Zn at these locations within the rat brain are consistent with other studies that utilized different analytical methodologies and both spatial and bulk analysis. This suggests that LA-ICP-MS can provide both spatial and quantitative elemental data for biological sections.

## References

1. Nagata T (2004) Prog Histochem Cytochem 39:185-319
2. Mesjasz-Przybylowicz J, Przybylowicz WJ (2002) Nucl Instrum Meth B 189:470–481
3. Chandra S (2003) Appl Surf Sci 203–204:679–683
4. Flinn JM, Hunter D, Linkous DH, Lanzirotti A, Smith LN, Brightwell J, Jones BF (2005) Physiol Behav 83:793–803

5. Punshon T, Jackson BP, Bertsch PM, Burger J (2004) J Environ Monitor 6:153–159
6. Hoffmann E, Ludke C, Skole J, Stephanowitz H, Ullrich E, Colditz D (2000) Fresenius J Anal Chem 367:579–585
7. Jackson BP, Hopkins WA, Baionno J (2003) Environ Sci Technol 37:2511–2515
8. Toland H, Perkins B, Pearce N, Keenan F, Leng MJ (2000) J Anal Atom Spectrom 15:1143–1148
9. Vander Putten E, Dehairs F, Keppens E, Baeyens W (2000) Geochim Cosmochim Ac 64:997–1011
10. Richardson CA, Chenery SRN, Cook JM (2001) Mar Ecol-Prog Ser 211:157–167
11. Watmough SA, Hutchinson TC, Evans RD (1998) J Environ Qual 27:1087–1094
12. Watmough SA, Hutchinson TC, Evans RD (1997) Environ Sci Technol 31:114–118
13. GarbeSchonberg CD, Reimann C, Pavlov VA (1997) Environ Geol 32:9–16
14. Feldmann J, Kindness A, Ek P (2002) J Anal Atom Spectrom 17:813–818
15. Kindness A, Sekaran CN, Feldmann J (2003) Clin Chem 49:1916–1923
16. Becker JS, Zoriy MV, Dehnhardt M, Pickhardt C, Zilles K (2005) J Anal Atom Spectrom 20:912–917
17. Becker JS, Zoriy MV, Pickhardt C, Palomero-Gallagher N, Zilles K (2005) Anal Chem 77:3208–3216
18. Durrant SF, Ward NL (2005) J Anal Atom Spectrom 20:821–829
19. Bush AI (2003) Trends Neurosci 26:207–214
20. Lovell MA, Robertson JD, Teesdale WJ, Campbell JL, Markesbery WR (1998) J Neurol Sci 158:47–52
21. Ren MQ, Ong WY, Makjanic J, Watt F (1999) Nucl Instrum Meth B 158:418–423
22. Mikhailova A, Davidson M, Channel JET, Guyodo Y, Batich C, Dobson J (2005) J Royal Soc Interface 2:33–37
23. Thong PSP, Watt F, Ponraj D, Leong SK, He Y, Lee TKY (1999) Nucl Instrum Methods Phys Res B 158:349–355
24. Robertson JD, Crafford AM, Markesbery WR, Lovell MA (2002) Nucl Instrum Methods Phys Res B 189:454–458
25. Becker JS, Zoriy M, Becker JS, Pickhardt C, Przybylski M (2004) J Anal Atom Spectrom 19:149–152
26. Becker JS, Zoriy M, Pickhardt C, Przybylski M, Becker JS (2005) Int J Mass Spectrom 242:135–144
27. Paxinos G, Watson C (1998) The rat brain in sterotaxic coordinates (4th edn) Academic Press, San Diego
28. Frederickson CJ, Kasarkis EJ, Ringo D, Frederickson RE (1987) J. Neurosci Methods 20:91–103
29. Speziali M, Orvini E (2003) Metals distribution and regionalization in the brain. In: Zatta P (ed) Metal ions in neurodegenerative diseases. World Scientific, Singanpore
30. Frederickson CJ, Klitenick MA, Manton WI, Kirkpatrick JB (1983) Brain Res 273:335–339
31. Tarohda T, Yamamoto M, Amano R (2004) Anal Bioanal Chem 280:240–246